J. Fluid Mech. (1985), *vol.* 160, *pp.* 447–463
Printed in Great Britain

The effect of large-eddy breakup devices on oncoming vorticity

By A. P. DOWLING
University Engineering Department, Trumpington Street, Cambridge CB2 1PZ

(Received 3 October 1984 and in revised form 1 May 1985)

Experiments have shown that a large-eddy breakup device consisting of a short splitter plate placed in the turbulent boundary layer over a plane wall can lead to a reduction in drag. We investigate the idealized problem of an incident line vortex convected past such a device. The vorticity shed from the trailing edge of the plate is found to cancel the effect of the incident vortex and to reduce velocity fluctuations significantly in the vicinity of the wall.

1. Introduction

Experiments have shown that large-eddy breakup devices, LEBUs or 'flow manipulators', consisting of short thin plates placed in the turbulent boundary layer above an extensive plane wall can reduce the drag per unit area on the wall. The geometry is illustrated in figure 1. The reduction in drag/unit area has been confirmed in a series of experiments performed independently by different groups of investigators (Hefner, Weinstein & Bushnell 1979; Corke, Guezennec & Nagib 1979; Corke, Nagib & Guezennec 1982; Hefner, Anders & Bushnell 1983; Mumford & Savill 1984). The effect seems to persist far downstream of the plate, and so, if the plane wall is sufficiently long in the streamwise direction and the plate is thin, the total drag on both the wall and the plate is less than that on the wall without the plate. Measurements have shown that flow manipulators reduce the large-scale velocity fluctuations in the turbulent boundary layer. Hefner *et al.* (1979) suggested that such a device might work by a process of 'vortex unwinding' in which a large-scale structure convected past the short plate generates a cancelling shed vortex. In this paper we investigate theoretically the effect of a plate on vortical structures in the flow and calculate the shed vorticity.

We consider a model problem which can be solved analytically. A thin plate is set at zero incidence to a uniform stream with uniform velocity U above an infinite plane surface. The flow is perturbed by a line vortex of strength Γ as shown in figure 2. The flow is two-dimensional, incompressible and inviscid, the only effect of viscosity being the application of the Kutta condition at the trailing edge of the plate. This means that vorticity is shed from the plate owing to the passage of the line vortex. The strength Γ of the vortex is assumed to be small, so that both the line vortex and the shed vorticity are convected with the stream velocity U.

Very simple arguments give an idea of the trends we can expect to see in the results. When the line vortex is upstream of the centreline of the plate it produces an upwash on the plate (see figure 2). Then, in order to move the stagnation point to the trailing edge and satisfy the Kutta condition, the circulation around the plate must be opposite in sign to Γ, and vorticity shed from the trailing edge has the same sign as the oncoming line vortex. However, once the line vortex has passed the centreline

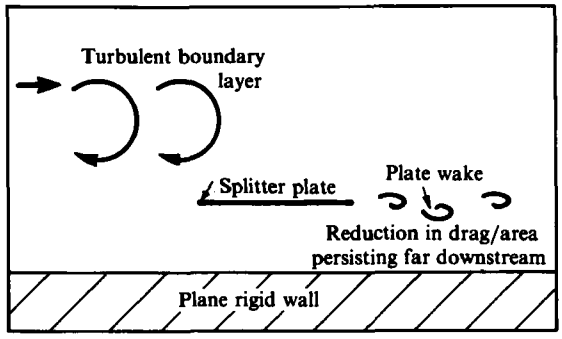

FIGURE 1. The geometry of a large-eddy breakup device consisting of a short plate in a turbulent wall boundary layer.

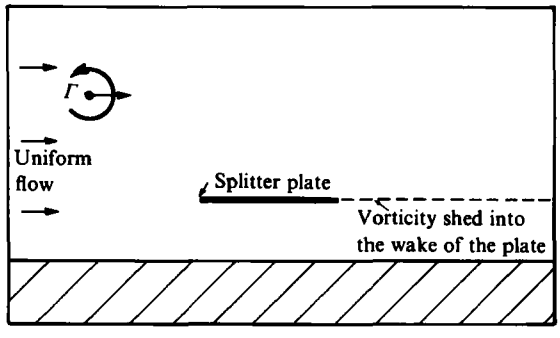

FIGURE 2. The idealized problem.

of the plate, it produces a downwash, shedding vorticity of opposite sign. Finally, as the vortex moves away the circulation around the plate reduces and vorticity with the same sign as Γ is shed again. This is a somewhat simplified view because it neglects the influence of the previously shed vorticity, but nevertheless it does give a reasonable physical interpretation of the more detailed results obtained in this paper.

The vorticity shed by the passage of a line vortex past an isolated plate is determined in §2. This is related to the classical problem of a sinusoidal gust convected past a thin aerofoil considered by many authors including Sears (1940), Graham (1970), Goldstein & Atassi (1976) and McKeogh & Graham (1980). Howe (1976) calculates the vorticity shed by the convection of a line vortex passed an isolated plate as a step in calculating the influence of vortex shedding on sound generation. He shows that the Fourier transform of the shed vorticity can be obtained quickly by the use of the von Kármán–Sears equation (von Kármán & Sears 1938). We obtain the same result by a different method – one that can also be used for the case of the plate above a plane infinite surface. We expand the vorticity distribution over the plate as a Glauert series. This method has been used extensively in unsteady aerodynamics, flutter and noise problems (see, e.g. Whitehead 1972; Goldstein 1976). Howe's result for the Fourier transform of the shed vorticity is recovered, and the transform inverted numerically to determine the time history of the shed vorticity. It is found that as the line vortex of strength Γ passes close to the trailing edge of the plate, a large amount of vorticity, opposite in sign to Γ, is shed. This vorticity convects downstream with the line vortex and significantly reduces its effect. The

magnitude of the cancelling vorticity depends on how close to the plate the vortex passes. If the vertical height of the vortex from the plate is 5% of the chord length, shed vorticity of strength $-0.8\,\Gamma$ is concentrated near the line vortex and effectively cancels it; if, however, the vortex height is 50% of the chord the cancelling vorticity is $-0.4\,\Gamma$. The calculations show that long after the passage of the line vortex the circulation around the plate is again zero, and so the total shed vorticity is zero, i.e. equal positive and negative amounts of vorticity are shed. The vorticity with the same sign as Γ is not concentrated. Therefore, while the plate does not change the total vorticity, it has the effect of considerably reducing its axial concentration, while increasing its axial extent. Liss & Usol'tsev (1973) used an approximate method to investigate the vorticity shed from a highly staggered set of thin plates due to the passage of a vortex. They also found considerable cancellation.

In §3 we go on to investigate the effect of a splitter plate above an infinite plane surface. The coefficients in the Glauert series now satisfy an infinite set of coupled equations. However, the higher-order coefficients decrease rapidly, and the series can be truncated to determine the Fourier transform of the shed vorticity. The vorticity is not significantly different from that shed from an isolated plate. The Fourier transform of the net velocity fluctuations far downstream of the plate is calculated. It is found that the flow manipulator significantly reduces the unsteady velocities near the wall for frequencies greater than U/chord length, provided the flow manipulator lies between the wall and incoming line vortex. For example, for a frequency of U/chord length the velocity fluctuation is reduced to about 50% of its amplitude without the plate; for frequencies above $4U$/chord length it is reduced by at least 80%. If, however, the line vortex passes between the plate and the wall little reduction in unsteadiness is obtained. Although the analysis is for a simplified model of a parallel-plate flow manipulator, it has led to a prediction that such a plate can significantly reduce large-scale velocity fluctuations. This agrees with experimental observations. As the momentum transport by the fluctuating Reynolds stress leads to large values of skin friction in a turbulent boundary layer, we can expect a reduction in fluctuating velocity to lead to a reduction in drag of the sort measured experimentally.

The theory is too simplified to give detailed predictions of optimal devices. Nevertheless, if we assume that the dominant velocity fluctuations in the wall boundary layer have frequencies of order $U/2\delta^*$ and higher, where δ^* is the boundary-layer displacement thickness and is approximately equal to one-eighth of the boundary-layer height δ, we conclude that a plate of length δ is required to produce a significant reduction in the velocity fluctuations. A longer plate would give little further reduction in these velocity fluctuations. This is consistent with experimental observations. The best position for the plate is found to be such that it lies between the wall and the oncoming vorticity. Once that constraint has been met a slight further improvement is obtained by having the plate as far away from the wall as possible.

2. Vortex shedding from an isolated plate

Consider a uniform flow parallel to a thin flat plate. We non-dimensionalize lengths so that the plate has a chord of length 2, and then choose a coordinate system such that the plate extends from $(-1, 0)$ to $(1, 0)$. A line vortex of strength Γ is at a height b above the plate as shown in figure 3. We linearize in the vortex strength Γ, and so the vortex convects with the mean flow. This will be a good approximation

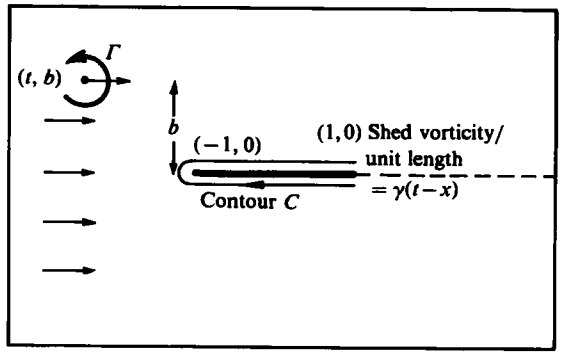

FIGURE 3. The geometry of the isolated plate.

provided Γ/bU is small in comparison with unity. Time is non-dimensionalized on the time taken for the vortex to travel a distance of half a chord. Then the mean velocity is $(1,0)$, and at time t the vortex is at position (t,b). As the line vortex convects past the plate vorticity is shed from the trailing edge to satisfy the Kutta condition. This shed vorticity is also convected with the mean velocity, and at time t we will denote the vorticity per unit length at a position x in the wake by $\gamma(t-x)$, $x > 1$.

The plate can be replaced by a distribution of vorticity $f(x,t)$, $-1 \leqslant x \leqslant 1$. $f(x,t)$ is equal to the jump in u, the x-component of velocity, across the plate,

$$f(x,t) = -[u(x,y,t)]_{y=0-}^{y=0+}, \tag{2.1}$$

and is to be determined from a condition of no normal velocity into the plate and the Kutta condition.

Kelvin's circulation theorem requires that the total circulation about the plate and its wake should vanish. Therefore the rate of change of circulation around the plate must be equal and opposite to the rate of vortex shedding. Hence

$$\frac{\mathrm{d}}{\mathrm{d}t}\int_{-1}^{1} f(x,t)\,\mathrm{d}x = -\frac{\mathrm{d}}{\mathrm{d}t}\int_{1}^{\infty} \gamma(t-x)\,\mathrm{d}x = -\gamma(t-1). \tag{2.2}$$

The Kutta condition states that there must not be a jump in pressure across the trailing edge of the plate:

$$[p(1,y,t)]_{y=0-}^{y=0+} = 0. \tag{2.3}$$

Now in this linearized problem $p = -\rho(\partial\phi/\partial t + u)$, and

$$[\phi(1,y,t)]_{y=0-}^{y=0+} = \int_C \nabla\phi\cdot\mathrm{d}\boldsymbol{x}, \tag{2.4}$$

where C is a contour surrounding the plate, as shown in figure 3. Hence the jump in ϕ across the trailing edge is equal and opposite to the circulation around the plate, and the condition (2.3) reduces to

$$\frac{\mathrm{d}}{\mathrm{d}t}\int_{-1}^{1} f(x,t)\,\mathrm{d}x = [u(1,y,t)]_{y=0-}^{y=0+} = -f(1,t). \tag{2.5}$$

A comparison with (2.2) therefore shows that the Kutta condition is equivalent to continuity of vorticity per unit length at $x = 1$:

$$f(1,t) = \gamma(t-1) = -\frac{\mathrm{d}}{\mathrm{d}t}\int_{-1}^{1} f(x,t)\,\mathrm{d}x. \tag{2.6}$$

The complex potential due to the line vortex, the plate and its wake is

$$w(z) = Uz - \frac{\mathrm{i}\Gamma}{2\pi}\ln(z-z_0) - \frac{\mathrm{i}}{2\pi}\int_{-1}^{1} f(x',t)\ln(z-x')\,\mathrm{d}x' - \frac{\mathrm{i}}{2\pi}\int_{1}^{\infty}\gamma(t-x')\ln(z-x')\,\mathrm{d}x', \tag{2.7}$$

where $z = x+\mathrm{i}y$ and $z_0 = t+\mathrm{i}b$. The condition of no flow into the plate gives

$$v(x,0) = 0 \quad (-1 \leqslant x \leqslant 1), \tag{2.8}$$

Differentiation of (2.7) shows that this is equivalent to

$$\Gamma\frac{(x-t)}{(x-t)^2+b^2} + \fint_{-1}^{1}\frac{f(x',t)}{x-x'}\,\mathrm{d}x' + \int_{1}^{\infty}\frac{\gamma(t-x')}{x-x'}\,\mathrm{d}x' = 0 \quad (-1 \leqslant x \leqslant 1). \tag{2.9}$$

$\fint$ denotes a principal value. We wish to solve (2.9) for f and γ, subject to the condition (2.6).

First we take Fourier transforms with respect to time, and introduce $\tilde{f}(x,\omega)$ and $\tilde{\gamma}(\omega)$, where

$$\tilde{f}(x,\omega) = \int_{-\infty}^{\infty} f(x,t)\,\mathrm{e}^{\mathrm{i}\omega t}\,\mathrm{d}t,$$

$$\tilde{\gamma}(\omega) = \int_{-\infty}^{\infty}\gamma(t)\,\mathrm{e}^{\mathrm{i}\omega t}\,\mathrm{d}t.$$

Since $\gamma(t)$ and $f(x,t)$ are real,

$$\tilde{\gamma}(-\omega) = \tilde{\gamma}^*(\omega), \quad \tilde{f}(x,-\omega) = \tilde{f}^*(x,\omega),$$

where the asterisk denotes a complex conjugate. We therefore only need consider positive real ω.

The Fourier transform of the condition (2.6) gives

$$\tilde{\gamma}\,\mathrm{e}^{\mathrm{i}\omega} = \tilde{f}(1,\omega) = \mathrm{i}\omega\int_{-1}^{1}\tilde{f}(x,\omega)\,\mathrm{d}x, \tag{2.10}$$

and from (2.9) we obtain

$$\fint_{-1}^{1}\frac{\tilde{f}(x',\omega)}{x-x'}\,\mathrm{d}x' = \mathrm{i}\pi\Gamma\,\mathrm{e}^{\mathrm{i}\omega x-\omega|b|} - \tilde{\gamma}(\omega)\int_{1}^{\infty}\frac{\mathrm{e}^{\mathrm{i}\omega x'}}{x-x'}\,\mathrm{d}x'. \tag{2.11}$$

This integral equation for $\tilde{f}$ has a Cauchy kernel and can be solved directly to give $\tilde{f}$ implicitly in terms of $\tilde{\gamma}$ (Carrier, Krook & Pearson 1966, p. 424). Use of (2.10) then leads to $\tilde{\gamma}$. Unfortunately this method does not extend in any simple way to the plate above a wall, so we adopt a different approach. We expand the function $\tilde{f}(x,\omega)$ as a Glauert series and write

$$\tilde{f}(x,\omega) = \tfrac{1}{2}(x+1)\tilde{f}(1,\omega) - \tfrac{1}{2}A_0(\omega)\cot\tfrac{1}{2}\theta + \sum_{m=1}^{\infty}A_m\sin m\theta, \tag{2.12}$$

where $\cos\theta = -x$. The A_0 term has the required form for the singularity at the leading edge. The first term on the right-hand side ensures that the contribution from the Fourier series vanishes at $x = 1$, $\theta = \pi$ and so improves the convergence of the series. Integration of this form with respect to x shows that

$$\int_{-1}^{1}\tilde{f}(x,\omega)\,\mathrm{d}x = \tilde{f}(1,\omega) + \tfrac{1}{2}\pi(A_1(\omega) - A_0(\omega)),$$

and hence from the condition (2.10),

$$\tilde{f}(1,\omega) = \tilde{\gamma}\,\mathrm{e}^{\mathrm{i}\omega} = \frac{\mathrm{i}\pi\omega}{2(1-\mathrm{i}\omega)}(A_1 - A_0). \tag{2.13}$$

Only the first two coefficients in the Glauert series need be calculated to determine the shed vorticity.

Substitution for $\tilde{f}(x,\omega)$ and $\tilde{\gamma}(\omega)$ into (2.11) gives

$$\fint_0^\pi \left\{-\tfrac{1}{2}A_0 \cot\tfrac{1}{2}\theta' + \sum_{m=1}^{\infty} A_m \sin m\theta'\right\} \frac{\sin\theta'\,\mathrm{d}\theta'}{\cos\theta' - \cos\theta} = \mathrm{i}\pi\Gamma\,\mathrm{e}^{-\mathrm{i}\omega\cos\theta - \omega|b|}$$
$$+ \frac{\mathrm{i}\pi\omega}{2(1-\mathrm{i}\omega)}(A_1 - A_0)\left\{\frac{1}{2}\fint_{-1}^{1} \frac{1+x'}{\cos\theta + x'}\,\mathrm{d}x' + \int_1^\infty \frac{\mathrm{e}^{\mathrm{i}\omega(x'-1)}}{\cos\theta + x'}\,\mathrm{d}x'\right\} \tag{2.14}$$

for $\omega > 0$. The integrals on the left-hand side can be evaluated in a straightforward way by replacing $2\sin m\theta'\sin\theta'$ by $\cos(m-1)\theta' - \cos(m+1)\theta'$ and using the Glauert integral

$$\fint_0^\pi \frac{\cos m\theta'}{\cos\theta' - \cos\theta}\,\mathrm{d}\theta' = \pi\frac{\sin m\theta}{\sin\theta}. \tag{2.15}$$

This gives

$$\tfrac{1}{2}A_0 + \sum_{m=1}^{\infty} A_m \cos m\theta = -\mathrm{i}\Gamma\,\mathrm{e}^{-\mathrm{i}\omega\cos\theta - \omega|b|}$$
$$- \frac{\mathrm{i}\omega(A_1 - A_0)}{2(1-\mathrm{i}\omega)}\left\{\frac{1}{2}\fint_{-1}^{1} \frac{(1+x')\,\mathrm{d}x'}{\cos\theta + x'} + \int_1^\infty \frac{\mathrm{e}^{\mathrm{i}\omega(x'-1)}}{\cos\theta + x'}\,\mathrm{d}x'\right\}. \tag{2.16}$$

The A_n can now be calculated by multiplying by $\cos n\theta$ and integrating from $\theta = 0$ to π. This leads to

$$A_n = -2\Gamma\mathrm{i}^{-n+1}J_n(\omega)\,\mathrm{e}^{-\omega|b|}$$
$$- \frac{\mathrm{i}\omega(A_1 - A_0)}{1-\mathrm{i}\omega}\left\{\frac{1}{2}\int_0^\pi (1-\cos\theta)\sin n\theta\,\mathrm{d}\theta + \int_1^\infty \frac{\mathrm{e}^{\mathrm{i}\omega(x'-1)}}{(x'^2-1)^{\frac{1}{2}}}[(x'^2-1)^{\frac{1}{2}} - x']^n\,\mathrm{d}x'\right\}. \tag{2.17}$$

We have used $J_n(\omega) = (\mathrm{i}^n/\pi)\int_0^\pi \cos n\theta\,\mathrm{e}^{-\mathrm{i}\omega\cos\theta}\,\mathrm{d}\theta$ (Abramowitz & Stegun 1964, p. 360) to evaluate the first term on the right-hand side. For the remaining two terms the orders of the θ and x' integrations have been exchanged. Then the Glauert integral (2.15) has been used to evaluate the second term in (2.17). The third term arises from an application of the standard integral

$$\int_0^\pi \frac{\cos n\theta}{\cos\theta + x'}\,\mathrm{d}\theta = \frac{\pi}{(x'^2-1)^{\frac{1}{2}}}[(x'^2-1)^{\frac{1}{2}} - x']^n \quad (x' > 1)$$

(Gradshteyn & Ryzhik 1965, p. 366).

To calculate the shed vorticity we need only evaluate A_0 and A_1. From (2.17)

$$A_0 = -2\Gamma\mathrm{i}J_0(\omega)\,\mathrm{e}^{-\omega|b|} + \frac{\pi\omega(A_1 - A_0)}{2(1-\mathrm{i}\omega)}H_0^{(1)}(\omega)\,\mathrm{e}^{-\mathrm{i}\omega}, \tag{2.18}$$

since $$\int_1^\infty \frac{\mathrm{e}^{\mathrm{i}\omega x'}}{(x'^2-1)^{\frac{1}{2}}}\,\mathrm{d}x' = \int_0^\infty \mathrm{e}^{\mathrm{i}\omega\cosh t}\,\mathrm{d}t = \tfrac{1}{2}\pi\mathrm{i}H_0^{(1)}(\omega).$$

Similarly $$\int_1^\infty \frac{\mathrm{e}^{\mathrm{i}\omega x'}}{(x'^2-1)^{\frac{1}{2}}}[(x'^2-1)^{\frac{1}{2}} - x']\,\mathrm{d}x' = -\frac{\mathrm{e}^{\mathrm{i}\omega}}{\mathrm{i}\omega} + \tfrac{1}{2}\pi H_1^{(1)}(\omega),$$

and so it follows from (2.17) that

$$A_1 = -2\Gamma J_1(\omega)\,\mathrm{e}^{-\omega|b|} - \frac{\mathrm{i}\omega(A_1 - A_0)}{1-\mathrm{i}\omega}\left\{\frac{\mathrm{i}\omega - 1}{\mathrm{i}\omega} + \tfrac{1}{2}\pi H_1^{(1)}(\omega)\,\mathrm{e}^{-\mathrm{i}\omega}\right\}. \tag{2.19}$$

Finally subtracting (2.18) from (2.19) gives

$$A_1 - A_0 = -4\Gamma\,\frac{1-\mathrm{i}\omega}{\mathrm{i}\pi\omega}\,\frac{J_0(\omega)+\mathrm{i}J_1(\omega)}{H_0^{(1)}(\omega)+\mathrm{i}H_1^{(1)}(\omega)}\,\mathrm{e}^{\mathrm{i}\omega-\omega|b|}. \tag{2.20}$$

From (2.13) the Fourier transform of the shed vorticity $\tilde{\gamma}$ is given by

$$\tilde{\gamma}(\omega) = -2\Gamma\,\frac{J_0(\omega)+\mathrm{i}J_1(\omega)}{H_0^{(1)}(\omega)+\mathrm{i}H_1^{(1)}(\omega)}\,\mathrm{e}^{-\omega|b|} \quad (\omega > 0). \tag{2.21}$$

This agrees with the expression obtained by Howe (1976, equation (3.25)). We see that the shed vorticity is an even function of b, and is therefore the same whether the vortex passes above or below the plate.

Inverting the Fourier transform to obtain the (x,t)-dependence of the shed vorticity we have $\gamma(t-x)$, the vorticity per unit length in the wake at position x and time t, given by

$$\begin{aligned}\gamma(t-x) &= \frac{1}{2\pi}\int_{-\infty}^{\infty}\tilde{\gamma}(\omega)\,\mathrm{e}^{-\mathrm{i}\omega(t-x)}\,\mathrm{d}t \\ &= \frac{1}{\pi}\int_0^{\infty}\{\cos\omega(t-x)\,\mathrm{Re}\,(\tilde{\gamma}(\omega)) + \sin\omega(t-x)\,\mathrm{Im}\,(\tilde{\gamma}(\omega))\}\,\mathrm{d}\omega,\end{aligned} \tag{2.22}$$

where we have used the fact that $\gamma(-\omega) = \gamma^*(\omega)$. $\tilde{\gamma}(\omega)$ for $\omega > 0$ is given in (2.21). This integral was evaluated numerically for $t = 5$, various axial positions x and three values of b. The results are shown in figure 4. At this time the line vortex is at position $(5,b)$. We see that there is a concentration of vorticity in the wake near the axial position of the line vortex but opposite in sign. Since $\gamma(t-x)$ is the vorticity per unit length of the wake, integrating it with respect to x in the vicinity of the line vortex demonstrates the effectiveness of the vorticity cancellation. The integral

$$\int_{x_1(t)}^{x_2(t)}\gamma(t-x)\,\mathrm{d}x$$

was evaluated numerically, where $x_1(t)$ and $x_2(t)$ are zeros of $\gamma(t-x)$ and $\gamma(t-x)/\Gamma < 0$ for $x_1(t) < x < x_2(t)$. This is the integral of the negative portions of the graphs in figure 4, and was found to be $-0.44\,\Gamma$ for $b = 1$, $-0.59\,\Gamma$ for $b = 0.5$ and $-0.81\,\Gamma$ for $b = 0.1$. In all cases the shed vorticity cancels a significant proportion of the vorticity in the incident line vortex, the cancellation being largest when the vortex passes closest to the plate. This vorticity cancellation was observed by Corke *et al.* (1982). Their flow visualisation showed that the passage of a large-scale structure induced vortex shedding of opposite sign from the trailing edge of a flat plate at zero incidence.

At large positive times the calculations show that the vorticity shed from the plate tends to zero. From the Kutta condition we would then expect there to be no circulation around the plate and hence be no net vorticity in the wake, i.e.

$$\int_1^{\infty}\gamma(t-x)\,\mathrm{d}x = 0 \tag{2.23}$$

for large enough values of t. We have already calculated the negative contribution to this integral for x in the range $x_1(t)$ to $x_2(t)$. Integration from 1 to $x_1(t)$ and from

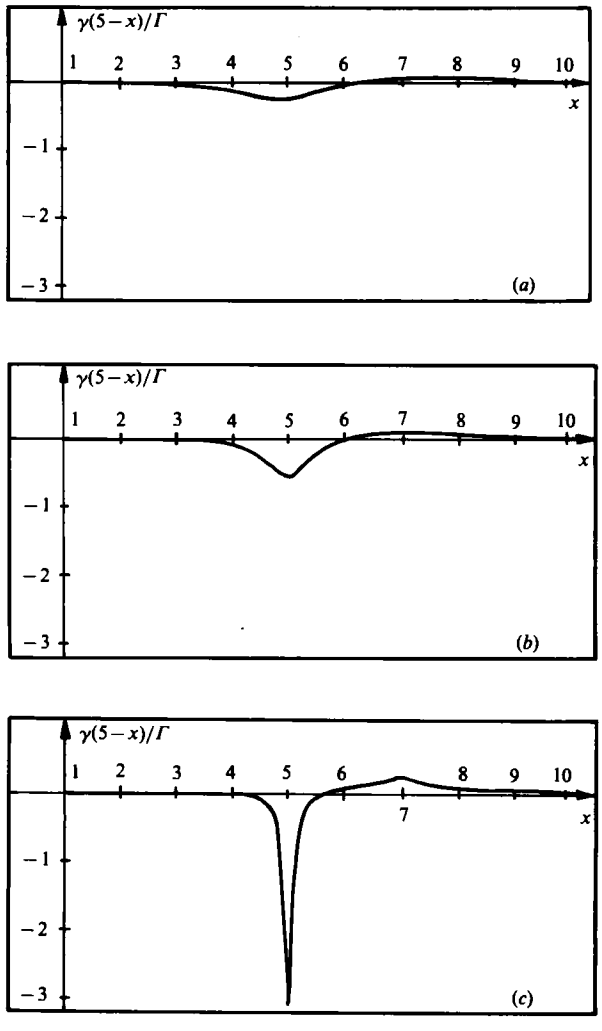

FIGURE 4. Plots of $\gamma(5-x)/\Gamma$, the shed vorticity/unit length of the wake at $t = 5$. At this time the line vortex of strength Γ is at position $(5, b)$. (*a*) $b = 1$; (*b*) 0.5; (*c*) 0.1.

$x_2(t)$ to infinity, where $\gamma(t-x)/\Gamma$ is positive, leads to a term that is equal and opposite to two significant figures, thereby proving that at large times there is no circulation around the plate and confirming (2.23). This provides a useful check on the accuracy of the numerical integration.

We have seen then that the passage of a line vortex of strength Γ past a plate leads to vortex shedding from the trailing edge of the plate, which tends to 'smear out' the total vorticity distribution. There is vorticity in the wake opposite in sign to Γ near the axial position of the line vortex, vorticity with the same sign being convected downstream well ahead of and behind the line vortex. We might expect such a vorticity distribution to produce less velocity fluctuations than an isolated line vortex. Eventually the incident vortex will interact nonlinearly with the nearby wake and 'roll-up'. This will further enhance the cancellation. In §3 we investigate a plate above a plane infinite wall, and find that the shed vorticity can significantly reduce the velocity fluctuations between the wake and the wall.

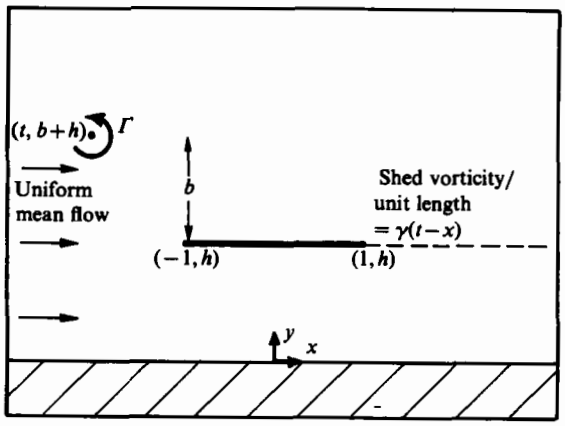

FIGURE 5. The idealized flow-manipulator geometry.

3. A vortex near a short plate above a plane infinite wall

Having determined the vorticity shed from an isolated plate due to the passage of a line vortex, we will now go on to investigate the influence of a nearby wall. This is the 'flow-manipulator' geometry in which a short thin plate is used to break up the large-scale eddies in the wall boundary layer. We consider a plate, again at zero incidence with a chord length of 2, positioned at a height h above an infinite hard plane surface, $y = 0$. As before we consider an incident line vortex convected with a uniform mean flow and at a non-dimensional height b above the plate, so that at time t the vortex is at position $(t, b+h)$. The geometry is illustrated in figure 5. Let $f(x,t)$ and $\gamma(t-x)$ again denote the vorticity per unit length for the plate and the wake: then, as in §2, Kelvin's circulation theorem and the Kutta condition give

$$f(1,t) = \gamma(t-1) = -\frac{\mathrm{d}}{\mathrm{d}t}\int_{-1}^{1} f(x,t)\,\mathrm{d}x \tag{3.1}$$

(cf. (2.6)).

The complex potential w is now given by

$$w(z) = Uz - \frac{\mathrm{i}\Gamma}{2\pi}\ln(z-z_0) + \frac{\mathrm{i}\Gamma}{2\pi}\ln(z-z_0^*) - \frac{\mathrm{i}}{2\pi}\int_{-1}^{1} f(x',t)\{\ln(z-z_1) - \ln(z-z_1^*)\}\,\mathrm{d}x'$$
$$- \frac{\mathrm{i}}{2\pi}\int_{1}^{\infty} \gamma(t-x')\{\ln(z-z_1) - \ln(z-z_1^*)\}\,\mathrm{d}x', \tag{3.2}$$

where $z_0 = t + \mathrm{i}(b+h)$, $z_1 = x' + \mathrm{i}h$ and the asterisk denotes a complex conjugate. The additional terms are due to the image of the vorticity distribution in the surface $y = 0$ and are required to give a flow satisfying no normal velocity into the hard surface. The condition of no flow into the plate gives

$$\Gamma\frac{x-t}{(x-t)^2+b^2} - \Gamma\frac{x-t}{(x-t)^2+(b+2h)^2} + \int_{-1}^{1} f(x',t)\left\{\frac{1}{x-x'} - \frac{x-x'}{(x-x')^2+4h^2}\right\}\mathrm{d}x'$$
$$+ \int_{1}^{\infty} \gamma(t-x')\left\{\frac{1}{x-x'} - \frac{x-x'}{(x-x')^2+4h^2}\right\}\mathrm{d}x' = 0 \tag{3.3}$$

for $-1 \leqslant x \leqslant 1$. As in §2, we solve this integral equation for f and γ by taking Fourier transforms with respect to time, and then substituting a Glauert series for $\hat{f}(x,\omega)$.

The Fourier transform of (3.3) gives

$$\int_{-1}^{1} \tilde{f}(x',\omega)\left\{\frac{1}{x-x'}-\frac{x-x'}{(x-x')^2+4h^2}\right\}\mathrm{d}x'+\tilde{\gamma}(\omega)\int_{1}^{\infty}\mathrm{e}^{\mathrm{i}\omega x'}\left\{\frac{1}{x-x'}-\frac{x-x'}{(x-x')^2+4h^2}\right\}\mathrm{d}x'$$
$$=\mathrm{i}\pi\Gamma\,\mathrm{e}^{\mathrm{i}\omega x}\{\mathrm{e}^{-\omega|b|}-\mathrm{e}^{-\omega(b+2h)}\} \quad (3.4)$$

for $-1\leqslant x\leqslant 1$. We now expand $\tilde{f}$ as a Glauert series

$$\tilde{f}(x,\omega)=\tfrac{1}{2}(x+1)\tilde{f}(1,\omega)-\tfrac{1}{2}A_0(\omega)\cot\tfrac{1}{2}\theta+\sum_{m=1}^{\infty}A_m(\omega)\sin m\theta,$$

with $\cos\theta=-x$. The condition (3.1) reduces to

$$\tilde{f}(1,\omega)=\tilde{\gamma}(\omega)\,\mathrm{e}^{\mathrm{i}\omega}=\frac{\mathrm{i}\pi\omega}{2(1-\mathrm{i}\omega)}[A_1(\omega)-A_0(\omega)]. \quad (3.5)$$

After replacing $\tilde{f}$ in (3.4) by the Glauert series, some terms can be simplified by using the Glauert integral

$$\int_0^{\pi}\frac{\cos m\theta'}{\cos\theta'-\cos\theta}\,\mathrm{d}\theta'=\pi\frac{\sin m\theta}{\sin\theta} \quad (3.6)$$

and by writing

$$E_m(x)=\frac{1}{\pi}\int_0^{\pi}\frac{\cos m\theta'(x+\cos\theta')}{(x+\cos\theta')^2+4h^2}\,\mathrm{d}\theta'. \quad (3.7)$$

$E_m(x)$ is evaluated in the Appendix. This leads to

$$\tfrac{1}{2}A_0[1-E_0(x)-E_1(x)]+\sum_{m=1}^{\infty}A_m[\cos m\theta+\tfrac{1}{2}E_{m-1}(x)-\tfrac{1}{2}E_{m+1}(x)]$$
$$-\frac{\mathrm{i}\omega(A_1-A_0)}{2(1-\mathrm{i}\omega)}\left\{\int_{-1}^{1}\frac{(1+x')}{2}\left[\frac{1}{x-x'}-\frac{x-x'}{(x-x')^2+4h^2}\right]\mathrm{d}x'\right.$$
$$\left.+\mathrm{e}^{-\mathrm{i}\omega}\int_1^{\infty}\mathrm{e}^{\mathrm{i}\omega x'}\left[\frac{1}{x-x'}-\frac{x-x'}{(x-x')^2+4h^2}\right]\mathrm{d}x'\right\}$$
$$=-\mathrm{i}\Gamma\,\mathrm{e}^{\mathrm{i}\omega x}\,[\mathrm{e}^{-\omega|b|}-\mathrm{e}^{-\omega(b+2h)}] \quad (3.8)$$

for $-1\leqslant x\leqslant 1$, $\cos\theta=-x$. We could determine A_n, $n=0,\ldots,N-1$, approximately by insisting that (3.8) be satisfied at N values of x. That is the approach adopted by Whitehead (1972) in a similar cascade problem. But instead, because such a procedure decouples the coefficients for the isolated plate, we will multiply (3.8) by $\cos n\theta$ and integrate from $\theta=0$ to π. This leads to an infinite number of coupled linear equations for the coefficients A_n:

$$A_n-A_0(C_{0,n}+C_{1,n})+\sum_{m=1}^{\infty}A_m(C_{m-1,n}-C_{m+1,n})+(A_0-A_1)S_n$$
$$=-2\Gamma\mathrm{i}^{-n+1}J_n(\omega)\,[\mathrm{e}^{-\omega|b|}-\mathrm{e}^{-\omega(2h+b)}] \quad (n\geqslant 0), \quad (3.9)$$

where
$$C_{m,n}=\frac{1}{\pi}\int_0^{\pi}\cos n\theta E_m(-\cos\theta)\,\mathrm{d}\theta. \quad (3.10)$$

$C_{m,n}$ was evaluated numerically using the analytical expression for E_m derived in the Appendix. $C_{m,n}$ is antisymmetric, which provides a useful check on the accuracy

of the numerical integration. In (3.9)

$$S_n = -\frac{\mathrm{i}\omega}{\pi(1-\mathrm{i}\omega)}\int_0^\pi \cos n\theta \left\{ \int_{-1}^{1} \frac{(1+x')}{2}\left[\frac{1}{\cos\theta+x'} - \frac{\cos\theta+x'}{(\cos\theta+x')^2+4h^2}\right]\mathrm{d}x' \right.$$
$$\left. + \mathrm{e}^{-\mathrm{i}\omega}\int_1^\infty \mathrm{e}^{\mathrm{i}\omega x'}\left[\frac{1}{\cos\theta+x'} - \frac{\cos\theta+x'}{(\cos\theta+x')^2+4h^2}\right]\mathrm{d}x' \right\}\mathrm{d}\theta. \quad (3.11)$$

After interchanging the order of the integrations in (3.11), the θ-integral can be evaluated to give

$$S_n = \frac{\mathrm{i}\omega}{1-\mathrm{i}\omega}\left\{-\frac{1}{2}\int_0^\pi (1-\cos\theta')\sin n\theta'\,\mathrm{d}\theta' + \frac{1}{2}\int_{-1}^{1}(1+x')\,E_n(x')\,\mathrm{d}x' \right.$$
$$\left. + \mathrm{e}^{-\mathrm{i}\omega}\int_1^\infty \mathrm{e}^{\mathrm{i}\omega x'}\left[E_n(x') - \frac{[(x'^2-1)^{\frac{1}{2}}-x']^n}{(x'^2-1)^{\frac{1}{2}}}\right]\mathrm{d}x'\right\}$$
$$= \frac{\mathrm{i}\omega}{1-\mathrm{i}\omega}\left\{s_n + \frac{1}{2}\int_{-1}^{1}(1+x')\,E_n(x')\,\mathrm{d}x' \right.$$
$$\left. + \mathrm{e}^{-\mathrm{i}\omega}\int_1^\infty \mathrm{e}^{\mathrm{i}\omega x'}\left[E_n(x') - \frac{[(x'^2-1)^{\frac{1}{2}}-x']^n}{(x'^2-1)^{\frac{1}{2}}}\right]\mathrm{d}x'\right\}, \quad (3.12)$$

where $s_0 = 0$, $s_1 = -1$, $s_n = [(-1)^n(2n^2-1)+1]/2n(n^2-1)$ for $n \geqslant 2$. The remaining integrals in S_n were evaluated numerically.

The only dependence on b, the height of the line vortex above the plate, is displayed explicitly on the right-hand side of (3.9). Therefore, instead of solving for A_n directly, we will determine $\hat{A}_n$, where

$$\hat{A}_n = \frac{A_n}{\Gamma[\mathrm{e}^{-\omega|b|} - \mathrm{e}^{-\omega(2h+b)}]}. \quad (3.13)$$

The $\hat{A}_n$ satisfy

$$\hat{A}_n - \hat{A}_0(C_{0,n}+C_{1,n}) + \sum_{m=1}^{\infty}\hat{A}_m(C_{m-1,n}-C_{m+1,n}) + (\hat{A}_0-\hat{A}_1)S_n$$
$$= -2\mathrm{i}^{-n+1}J_n(\omega) \quad (n \geqslant 0), \quad (3.14)$$

and are independent of b, being functions of ω and h only. The $\hat{A}_n$ decay rapidly as n becomes large, and so we can solve (3.14) approximately by truncating the series after N terms, and solving the first N equations in (3.14) for the N unknowns $\hat{A}_0, \ldots, \hat{A}_{N-1}$. The Fourier transform of the shed vorticity can then be calculated from (3.5):

$$\tilde{\gamma}(\omega) = \hat{\gamma}(\omega)\,\Gamma[\mathrm{e}^{-\omega|b|} - \mathrm{e}^{-\omega(2h+b)}], \quad (3.15)$$

where

$$\hat{\gamma}(\omega) = \frac{\mathrm{i}\pi\omega}{2(1-\mathrm{i}\omega)}(\hat{A}_1-\hat{A}_0)\,\mathrm{e}^{-\mathrm{i}\omega} \quad (3.16)$$

and is independent of b. $\tilde{\gamma}(\omega)$ was determined by truncating the Glauert series after 8 and after 12 terms. The two results agreed to six significant figures, thereby verifying the validity of the procedure.

Figure 6 shows plots of $\tilde{\gamma}(\omega)$ for $b = 0.1$ and three values of h. The Fourier transform of the vorticity shed from the isolated plate (given in (2.21)) is also shown for comparison. We see that for $\omega h > 2$ the nearby wall has very little effect on the shed vorticity.

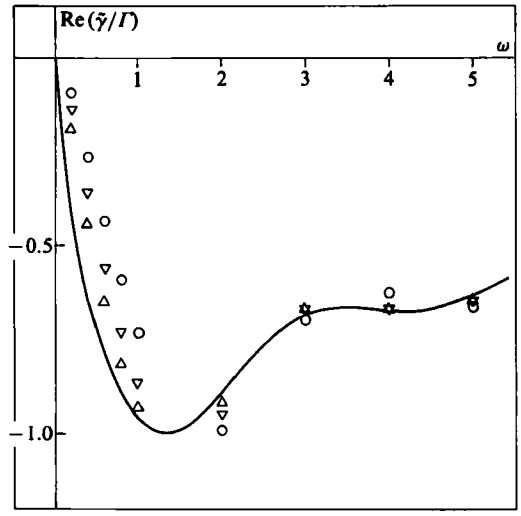

FIGURE 6. Plots of the real part of the Fourier transform of the shed vorticity, Re $(\tilde{\gamma}(\omega))$, versus frequency ω for $b = 0.1$, and $h = 0.1$ (○), 0.5 (▽), 1.0 (△). The line is the real part of the vorticity shed from an isolated plate with $b = 0.1$.

As the line vortex is convected past the plate, vorticity of opposite sign is shed from the trailing edge of the plate. Equations (3.15) and (3.16) give the Fourier transform of this shed vorticity. In order to quantify the cancelling effect of the vortex shedding we will calculate the Fourier transform of the velocity fluctuations near the wall downstream of the plate.

The fluid velocity can be determined from the complex potential given in (3.2). For example the Fourier transform of the x-component of the fluctuating velocity, $\tilde{u}(x, y, \omega)$, is given by

$$\begin{aligned}\tilde{u}(x,y,\omega) = {} & \tfrac{1}{2}\Gamma\, \mathrm{e}^{\mathrm{i}\omega x-\omega(h+b)}\,[\mathrm{e}^{\omega y}+\mathrm{e}^{-\omega y}] \\ & -\frac{\tilde{\gamma}(\omega)}{2\pi}\int_1^\infty \mathrm{e}^{\mathrm{i}\omega x'}\left\{\frac{y-h}{(x-x')^2+(y-h)^2}-\frac{y+h}{(x-x')^2+(y+h)^2}\right\}\mathrm{d}x' \\ & -\frac{1}{2\pi}\int_{-1}^{1} f(x',\omega)\left\{\frac{y-h}{(x-x')^2+(y-h)^2}-\frac{y+h}{(x-x')^2+(y+h)^2}\right\}\mathrm{d}x' \qquad (3.17)\end{aligned}$$

for a height y below the path of the line vortex, so that $h+b-y$ is positive. The first two terms in (3.17) describe the x-component of the velocity fluctuations induced by the incident vortex and the wake, and do not decay as x tends to $+\infty$. The last term describes the local effect of the circulation around the plate and decays rapidly (like $(x-1)^{-2}$) as x becomes large and positive. Hence for positions a reasonable distance downstream of the plate the third integral is negligible and the second can be evaluated. For a position below both the plate and the path of the line vortex, $\tilde{u}$ simplifies to

$$\tilde{u}(x,y,\omega) = \tfrac{1}{2}\Gamma\, \mathrm{e}^{\mathrm{i}\omega x-\omega(h+b)}\,[\mathrm{e}^{\omega y}+\mathrm{e}^{-\omega y}]\left[1+\frac{\tilde{\gamma}(\omega)\,\mathrm{e}^{\omega b}}{\Gamma}\right]. \qquad (3.18)$$

Without the splitter plate the velocity fluctuation produced by the passage of the line vortex and its image would be given by

$$\tilde{u} = \tfrac{1}{2}\Gamma\, \mathrm{e}^{\mathrm{i}\omega x-\omega(h+b)}\,[\mathrm{e}^{\omega y}+\mathrm{e}^{-\omega y}]. \qquad (3.19)$$

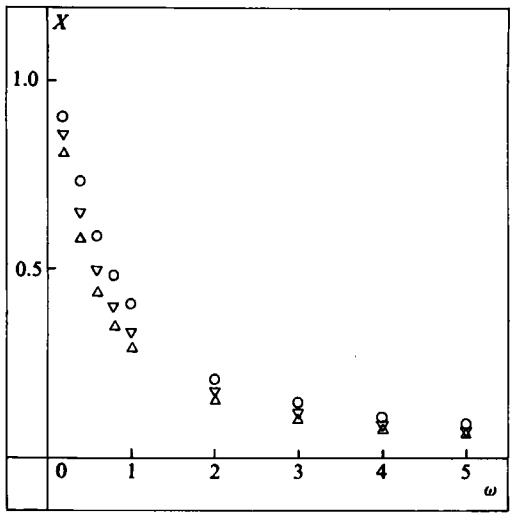

FIGURE 7. Plots of $X = |1+\tilde{\gamma}(\omega)\,e^{\omega b}/\Gamma|$ versus frequency ω for positive b and $h = 0.1$ (○), 0.5 (▽), 1.0 (△). $|1+\tilde{\gamma}(\omega)\,e^{\omega b}/\Gamma|$ is the ratio between the magnitude of the velocity fluctuations near the wall with and without the flow manipulator.

We see then that the presence of the flow manipulator reduces the Fourier transform of the streamwise fluctuating velocities by a factor

$$1+\frac{\tilde{\gamma}(\omega)\,e^{\omega b}}{\Gamma}.$$

The Fourier transform of the fluctuating vertical velocity can be calculated in a similar way, and for large x, y less than $h+b$ and h, is given by

$$\tilde{v}(x,y,\omega) = -\tfrac{1}{2}i\Gamma\,e^{i\omega x-\omega(h+b)}\,[e^{\omega y}-e^{-\omega y}]\left[1+\frac{\tilde{\gamma}(\omega)\,e^{\omega b}}{\Gamma}\right]. \tag{3.20}$$

Again the velocity has been reduced by a factor $1+\tilde{\gamma}(\omega)\,e^{\omega b}/\Gamma$ by the presence of the splitter plate.

Plots of $|1+\tilde{\gamma}(\omega)\,e^{\omega b}/\Gamma|$ are shown in figures 7 and 8. The dependence on b, the height of the incident line vortex above the plate, is particularly simple, and so we will investigate it analytically before discussing the graphs in detail. From (3.15)

$$1+\frac{\tilde{\gamma}(\omega)\,e^{\omega b}}{\Gamma} = 1+\hat{\gamma}(\omega)\,[e^{\omega(b-|b|)}-e^{-2\omega h}]. \tag{3.21}$$

where $\hat{\gamma}(\omega)$ is given in (3.16) and is independent of b. We see then that any positive value of b gives the same percentage reduction in velocity, but a negative b is far less effective. In other words, for a significant cancellation of velocity fluctuations in the vicinity of the wall, we require the plate to lie between the position of the incident vortex and the wall. We can explain this quite simply. In the Fourier-transformed problem the convected vortex of strength Γ is smeared out into a vortex sheet of strength $\Gamma\,e^{i\omega x}$. The velocity fluctuations induced by such a vorticity distribution decay like $e^{-\omega d}$, where d is the distance away from the sheet. Disturbances in the vicinity of the plate are therefore of order $e^{-\omega|b|}$, and so the strength of the shed vorticity is also proportional to $e^{-\omega|b|}$. At a position y below both the incident vortex and the plate the velocity perturbation due to the incident vorticity is proportional

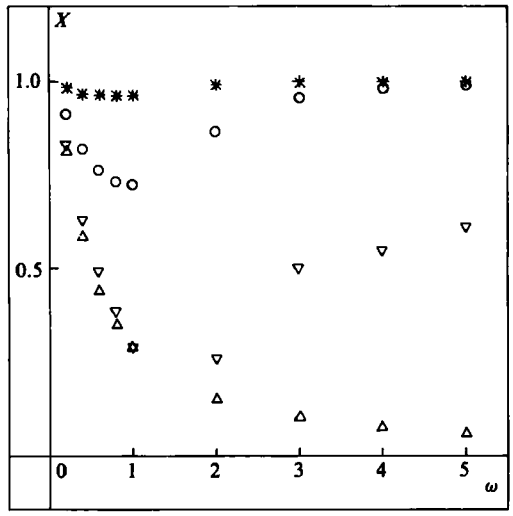

FIGURE 8. Plots of $X = |1+\tilde{\gamma}(\omega)\,e^{\omega b}/\Gamma|$ versus frequency ω for $h = 1$ and $b = -0.9$ (*), -0.5 (○), -0.1 (∇), $b > 0$ ($\triangle$). $|1+\tilde{\gamma}(\omega)\,e^{\omega b}/\Gamma|$ is the ratio between the velocity fluctuations near the wall with and without the flow manipulator. Far less reduction is obtained for negative values of b.

to $e^{-\omega(b+h-y)}$ and that due to the shed vorticity is proportional to $e^{-\omega|b|}\,e^{-\omega(h-y)}$. We see, then, that if b is positive these two effects are of the same order and we can have efficient cancellation. If, however, b is negative, the effect of incident vorticity is larger than that of the shed vorticity and the cancellation will be less dramatic. These conclusions are demonstrated in the numerical calculations.

Figure 7 shows the variation of $|1+\tilde{\gamma}(\omega)\,e^{\omega b}/\Gamma|$ with ω for all positive b and three different values of h. This is the ratio between the magnitude of velocity fluctuations of frequency ω near the wall with and without the splitter plate. We see that for $\omega = 0.5$ the velocity fluctuations are reduced by about 50 %, while for ω greater than 2 the reduction exceeds 80 %. This is in agreement with the experimental observation that flow manipulators reduce large-scale velocity fluctuations. We might expect this decrease in flow perturbation to lead to a corresponding reduction in skin friction, because the transport of momentum by vertical velocity fluctuations induced by eddies leads to a significant proportion of the skin friction in a turbulent boundary layer. We have seen that the flow manipulator very effectively reduces vertical velocity fluctuations near the wall for positive b and non-dimensional frequencies greater than about 2. We have non-dimensionalized time on $l/2U$, where l is the plate length and U the free-stream velocity. Therefore we have efficient cancellation for dimensional frequencies greater than $4U/l$. If the dominant disturbances in the wall boundary layer have frequencies greater than or equal to $U/2\delta^*$, where δ^* is the boundary-layer displacement thickness and is approximately one-eighth of the boundary-layer height, we can expect them to be effectively cancelled by a plate whose length l exceeds δ. Hefner *et al.* (1983) found a plate whose length was approximately equal to the boundary-layer height gave optimal results, with shorter plates having little effect on the turbulent boundary and longer plates having an increased device drag.

Figure 8 shows the fractional reduction in the magnitude of velocity fluctuations near the wall for negative b. As we expected from the analytical form, the device is far less effective. We therefore conclude that the splitter plate should be positioned so that it lies between the oncoming vortices and the wall. Figure 7 shows that h,

the height of the plate above the wall, has a slight effect on the reduction of velocity fluctuations, with larger values of h being more effective. This implies that the optimal position of the plate would be so that it is between the wall and the vorticity in the large-scale structure, but as far from the wall as possible, given that constraint.

4. Conclusions

We have found that the passage of a vortex over a splitter plate leads to the shedding of vorticity of opposite sign from the trailing edge. This can lead to a significant reduction in the fluctuating velocity in the vicinity of a hard wall if the plate is positioned between the incident vortex and the wall.

It is a pleasure to thank Dr T. P. Hynes for his helpful comments. The work has been carried out with the support of Topexpress Ltd and the Procurement Executive, Ministry of Defence.

Appendix

Integrals of the form

$$E_n(x) = \frac{1}{\pi}\int_0^{\pi} \frac{\cos n\theta(\cos\theta + x)}{(\cos\theta + x)^2 + 4h^2}\,\mathrm{d}\theta \tag{A 1}$$

arise frequently in this work. We will calculate $E_n(x)$ by considering $D_n(x)$, where

$$D_n(x) = \frac{1}{2\pi}\int_0^{2\pi} \frac{\cos n\theta}{\cos\theta + x + 2\mathrm{i}h}\,\mathrm{d}\theta; \tag{A 2}$$

$E_n(x)$ is equal to the real part of $D_n(x)$.

D_0 can be evaluated in a standard way by contour integration. With $z = \mathrm{e}^{\mathrm{i}\theta}$,

$$D_0(x) = \frac{1}{\pi\mathrm{i}}\oint \frac{\mathrm{d}z}{z^2 + 2z(x + 2\mathrm{i}h) + 1}. \tag{A 3}$$

The integral is to be evaluated around the unit circle, giving

$$D_0(x) = \frac{2}{z_1 - z_1^{-1}}, \tag{A 4}$$

where z_1 is the root of the quadratic equation $z^2 + 2z(x + 2\mathrm{i}h) + 1 = 0$ with modulus less than 1. z_1^{-1} is then the other root, and

$$z_1 = -x - 2\mathrm{i}h + z_2, \quad \text{where } z_2 = [(x + 2\mathrm{i}h)^2 - 1]^{\frac{1}{2}}, \tag{A 5}$$

with the sign of the square root being chosen such that $|z_1| < 1$. Substituting for z_1 in (A 4), we find that

$$D_0(x) = \frac{1}{z_2}. \tag{A 6}$$

Now

$$\begin{aligned} D_1(x) &= \frac{1}{2\pi}\int_0^{2\pi} \frac{\cos\theta}{\cos\theta + x + 2\mathrm{i}h}\,\mathrm{d}\theta \\ &= \frac{1}{2\pi}\int_0^{2\pi} \mathrm{d}\theta - (x + 2\mathrm{i}h)\,D_0(x). \end{aligned}$$

Hence

$$D_1(x) = \frac{z_2 - x - 2\mathrm{i}h}{z_2}. \tag{A 7}$$

We speculate that $D_n = (z_2 - x - 2ih)^n / z_2$. Equations (A 6) and (A 7) show that this is true for $n = 0$ and 1. We will prove it for general n by induction. Suppose

$$D_m(x) = \frac{(z_2 - x - 2ih)^m}{z_2} \quad (m \leqslant n). \tag{A 8}$$

Then

$$D_{n+1}(x) = \frac{1}{2\pi} \int_0^{2\pi} \frac{\cos n\theta \cos\theta - \sin n\theta \sin\theta}{\cos\theta + x + 2ih} \, d\theta$$

$$= -(x + 2ih) D_n(x) + \tfrac{1}{2} D_{n+1}(x) - \tfrac{1}{2} D_{n-1}(x),$$

i.e.

$$D_{n+1}(x) = -2(x + 2ih) D_n(x) - D_{n-1}(x). \tag{A 9}$$

We can use (A 8) to replace $D_n(x)$ and $D_{n-1}(x)$ in (A 9). After some algebra, this leads to

$$D_{n+1}(x) = (z_2 - x - 2ih)^{n+1} / z_2, \tag{A 10}$$

thus completing the proof by induction. Hence

$$E_n(x) = \mathrm{Re}\left\{\frac{1}{z_2} (z_2 - x - 2ih)^n\right\} \tag{A 11}$$

for $n \geqslant 0$, where $z_2 = [(x + 2ih)^2 - 1]^{\frac{1}{2}}$, the sign of the root being chosen such that $|-x - 2ih + z_2| < 1$.

REFERENCES

Abramowitz, M. & Stegun, I. A. 1965 *Handbook of Mathematical Functions*. Dover.

Carrier, G. F., Krook, M. & Pearson, C. E. 1966 *Functions of a Complex Variable: Theory and Technique*. McGraw-Hill.

Corke, T. C., Guezennec, Y. G. & Nagib, H. M. 1979 Modification in drag of turbulent boundary layers resulting from manipulation of large-scale structures. In *Proc. Viscous Drag Reduction Symp., Dallas. AIAA Prog. Astro. Aero.* **72**, 128–143.

Corke, T. C., Nagib, H. M. & Guezennec, Y. G. 1982 A new view on origin, role and manipulation of large scales in turbulent boundary layers. *NASA CR* 165861.

Goldstein, M. E. 1976 *Aeroacoustics*, p. 229. McGraw-Hill.

Goldstein, M. E. & Atassi, H. 1976 A complete second-order theory for the unsteady flow about an airfoil due to a periodic gust. *J. Fluid Mech.* **74**, 741–765.

Gradshteyn, I. S. & Ryzhik, I. M. 1965 *Tables of Integrals, Series and Products*. Academic.

Graham, J. M. R. 1970 Lifting surface theory for the problem of an arbitrarily yawed sinusoidal gust incident on a thin aerofoil in incompressible flow. *Aero. Q.* **21**, 182–198.

Hefner, J. N., Weinstein, L. M. & Bushnell, D. M. 1979 Large-eddy break-up scheme for turbulent viscous drag reduction. In *Proc. Viscous Drag Reduction Symp., Dallas. AIAA Prog. Astro. Aero.* **72**, 110–127.

Hefner, J. N., Anders, J. B. & Bushnell, D. M. 1983 Alteration of outer flow structures for turbulent drag reduction. *AIAA*-8300293.

Howe, M. S. 1976 Influence of vortex shedding on sound generation. *J. Fluid Mech.* **76**, 711–740.

Liss, A. Yu. & Usol'tsev, A. A. 1973 Influence of vortex–wing interaction on reducing vortex induction. *Izv. Aviatsionnaya Tecknika* **16**, 5–10.

Kármán, T. von & Sears, W. R. 1938 Airfoil theory for non-uniform motion. *J. Aero. Sci.* **5**, 379–390.

McKeogh, P. J. & Graham, J. M. R. 1980 The effect of mean loading on the fluctuating loads induced on aerofoils by a turbulent stream. *Aero. Q.* **31**, 56–69.

MUMFORD, J. C. & SAVILL, A. M. 1984 Parametric studies of flat plate, turbulence manipulators including direct drag results and laser flow visualisation. In *Laminar and Turbulent Boundary Layers. Proc. ASME Energy Sources Technology Conference, New Orleans, 12–16 February 1984* (eds. E. M. Uram & H. E. Weber), pp. 41–51.

SEARS, W. R. 1940 Some aspects of non-stationary airfoil theory and its practical application. *J. Aero. Sci.* **8**, 104–108.

WHITEHEAD, D. S. 1972 Vibration and sound generation in a cascade of flat plates in subsonic flow. *Aero. Res. Counc. R & M* 3685.